

Transport properties of sharp antiferromagnetic boundaries in Gd/Fe multilayers

José L. Prieto,* Bas B. van Aken, Gavin Burnell, Chris Bell, Jan E. Evetts, Neil Mathur, and Mark G. Blamire

Department of Materials Science and Metallurgy, University of Cambridge, Pembroke Street, Cambridge, CB2 3QZ, United Kingdom

(Received 12 September 2003; revised manuscript received 30 October 2003; published 27 February 2004)

The transport properties of sharp antiferromagnetic boundaries between Gd and Fe have been studied. The measurements were carried out with the current perpendicular to the plane at 20 K and up to 8 T in multilayer Gd/Fe of different thicknesses. We have extended the Valet and Fert model for giant magnetoresistive multilayers to explain the results in terms of spin-dependent scattering at the interface that changes its magnitude when the external field decreases the angle of the interface.

DOI: 10.1103/PhysRevB.69.054436

PACS number(s): 72.25.Mk, 72.25.Rb, 75.70.Cn

Spin-polarized transport in ferromagnetic metals is the key to understanding most of the systems involving giant magnetoresistance (GMR). Although multilayers of ferromagnetic (FM)/nonmagnetic (NM) materials are quite well characterized, multilayers of FM/FM are not so well understood. In particular, when the two ferromagnetic layers couple antiferromagnetically at the interface, the spin transport can provide valuable information for understanding other MR systems.

Recently Eerenstein *et al.*¹ reported on sharp antiferromagnetic boundaries in Fe_3O_4 . This system presents disordered dislocations that constitute antiferromagnetic boundaries. The number and shape of the boundaries cannot be determined; therefore a quantitative analysis of spin transport cannot be done. In the system described in this paper, with multilayers of Gd/Fe antiferromagnetically coupled, the number of interfaces is exactly known. Also, in the current perpendicular to plane (CPP) geometry,² with all the boundaries perpendicular to the current, we avoid unwanted effects such as anisotropic magnetoresistance (AMR) that could obscure the correct interpretation of the results. In this paper we show that the Valet and Fert³ model for GMR structures can explain the behavior of sharp antiferromagnetic boundaries in an applied magnetic field and thus give us a good understanding of spin diffusion and scattering at these interfaces.

Gadolinium couples antiferromagnetically with transition metals. Gd/Fe (Refs. 4, 6) is a system of particular interest in this study because the interface is quite sharp and the layers do not interdiffuse,⁵ unlike in Gd/Co (Ref. 6) or Gd/Ni.⁷ Almost all the work reported to date on the transport and magnetic properties of Gd/Fe multilayers is based on polycrystalline samples. This type of sample shows a very sharp interface with ~ 2 nm of amorphous Fe (arising from the large lattice mismatch) before this layer become polycrystalline.⁵ Gadolinium is a ferromagnet with a Curie temperature of 293 K and a high moment of $7.55\mu_B$ at 10 K. At low temperatures, a multilayer of Gd/Fe is an antiferromagnetic structure where all the Gd layers point in one direction and the Fe layers are rotated by 180° . When an external field is applied to a simple bilayer of Gd/Fe at low temperatures, the Gd aligns with the field because its higher moment and the Fe layers align antiparallel to the Gd and the field. At higher fields (for example, over 0.4 kOe at 10 K), the interface moments start to rotate away from the field to minimize Zeeman energy to form the so-called “twisted

state.”⁸ The field necessary to achieve this twisted state depends on the difference between the moments in Gd and in Fe (and on the temperature) and it will decrease when the moments of both materials become similar. The behavior of a multilayer is very similar to that of the bilayer, although not identical, as will be explained in more detail later.

The samples used in our study are sputtered multilayers with n bilayers of Gd/Fe plus one Fe layer on top, deposited at room temperature on Si 100 with a Cu buffer layer (also bottom contact) as described below. The samples have a 10 nm Au capping layer to prevent oxidation during the processing. The thickness of each layer is varied from sample to sample. The base pressure was $< 10^{-8}$ mbar and the deposition rates were 0.16 nm/s for Fe and 0.4 nm/s for Gd. X-ray measurements show a polycrystalline sample with a grain size of ~ 6 nm as was expected from the deposition conditions.⁹

In order to maximize the measured signal, the sample was patterned with a standard lift-off process into arrays of 476 mesas ($10\ \mu\text{m} \times 10\ \mu\text{m}$ each) connected in series by Cu wiring layers ($\rho_{\text{Cu}} \sim 3\ \mu\Omega\ \text{cm}$ at room temperature). A SiO_2 layer prevents the top Cu contacts shorting the sidewalls of the mesas (see dimensions in Fig. 1). The Cu deposition was carried out after Ar ion milling to improve the contact resistance. Two of these arrays were connected in a Wheatstone bridge configuration with a further two arrays of 476 connections in series without the multilayer mesas (Fig. 1); the resistance of these latter arrays is due only to the Cu contacts, thus the bridge geometry minimizes the contribution of the Cu wiring to the final measurement of the resistance of the contacts. Despite all these precautions there is still some additional resistance due to the Cu contact; this is discussed later. It is clear from Fig. 1 that the current is flowing perpendicular (CPP) to the layers and the interfaces. This geometry avoids any contribution from AMR because the current is always perpendicular to the magnetization.

The samples studied were $\text{Fe}_{30\ \text{nm}}(\text{Gd}_{30\ \text{nm}}\text{Fe}_{30\ \text{nm}})_6$, $\text{Fe}_{5\ \text{nm}}(\text{Gd}_{30\ \text{nm}}\text{Fe}_{5\ \text{nm}})_6$, $\text{Fe}_{30\ \text{nm}}(\text{Gd}_{5\ \text{nm}}\text{Fe}_{30\ \text{nm}})_6$, and $\text{Fe}_{5\ \text{nm}}(\text{Gd}_{5\ \text{nm}}\text{Fe}_{5\ \text{nm}})_{30}$, processed as described above. Figure 2 shows the hysteresis loops of the films at 20 K measured in a vibrating sample magnetometer (VSM). This graph shows the samples $\text{Gd}_{5\ \text{nm}}\text{-Fe}_{30\ \text{nm}}$ and $\text{Gd}_{5\ \text{nm}}\text{-Fe}_{5\ \text{nm}}$, where a large part of the total magnetization is involved in the twisted state. In the other two samples, most of the magnetization is

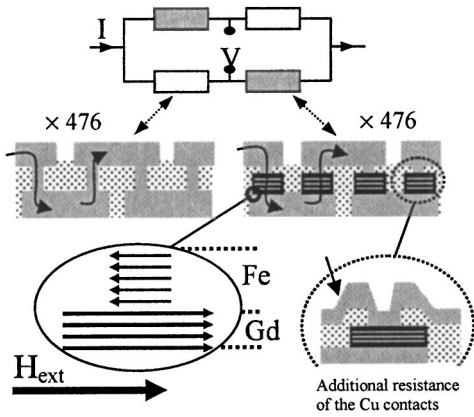


FIG. 1. A Wheatstone bridge configuration has been used to minimize the contribution to the resistance coming from the Cu contacts. Two of the resistors are 476 multilayer (Gd/Fe)_n mesas connected in series with Cu contacts (300 nm thick). The other two resistors are 476 connections without the multilayer, only the resistance of the Cu. There is an insulator SiO₂ layer (350 nm thick) that protects the mesas from shorting together. The window of the SiO₂ over every mesa is 3.5×3.5 μm². The bottom left inset shows the magnetic configuration at the Gd-Fe interface for zero field. The bottom right inset shows the possible origin of the extra-resistance of the Cu contacts, where the Cu overlaps the SiO₂ window (note that in the arms without the multilayer this overlap is not present).

aligned with the field in almost all the field range and therefore the twisted state cannot be discerned in the hysteresis loop.

The quality of the interface was analyzed by low angle x-ray reflectivity (also used to confirm the thicknesses of the layers) and AFM scans at different stages of the deposition. Figure 3 shows an example for the Gd_{5 nm}-Fe_{30 nm} multilayer. X-ray reflectivity gives a value of roughness at the interfaces always lower than 0.45 nm. The AFM scans give a mean average roughness lower than 0.5 Å over an area of 3 μm × 3 μm (the maximum value found, 0.63 nm, is shown in the

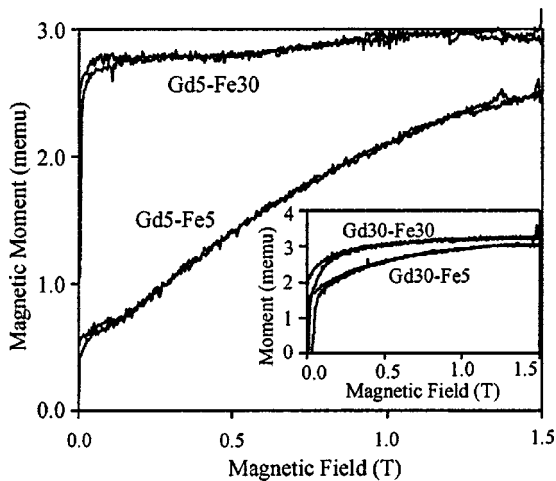


FIG. 2. Approach to saturation of the hysteresis loops of the four samples under study. The samples with a higher percentage of moment involved in the twisted spring show a larger continuous increase in magnetization with increasing field even at high fields.

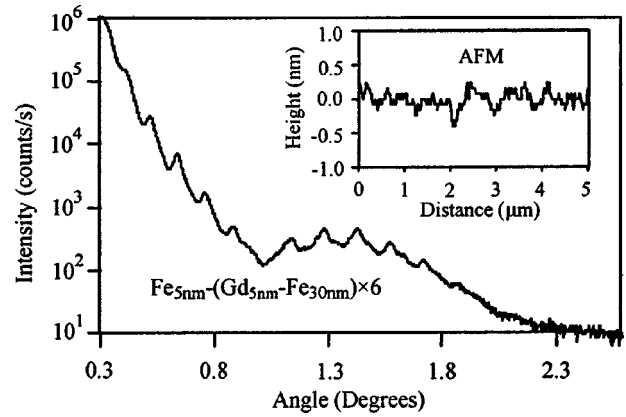


FIG. 3. Low angle x-ray reflectivity for one of the samples Fe_{5 nm}-(Gd_{5 nm}-Fe_{30 nm})×6. This technique was used to check the thickness of the layers and estimate the roughness of the interface. The inset shows cross sections of an AFM image taken at the top of the multilayer showing the maximum roughness found (0.62 nm peak to peak) and the long-range nature of the roughness.

cross section of the inset of Fig. 3). It also shows long-range roughness (“orange peel” type) of ~3 Å and an average period of ~500 nm.

We can estimate the total resistance of each sample with the values of resistivities of the films. These values were obtained from measurements in equivalent films with the current in plane at 20 K and are $\rho_{\text{Gd}} = 110 \mu\Omega \text{ cm}$ and $\rho_{\text{Fe}} = 8 \mu\Omega \text{ cm}$. These are standard values for thin films, much higher than the bulk values at the same temperature. Similar values were used in previous AMR transport studies with the current-in-plane in Gd/Fe multilayers.¹⁰ The calculated resistances are 8.3, 7.8, 1.9, and 6.9 Ω for the samples with Gd_{30 nm}Fe_{30 nm}, Gd_{30 nm}Fe_{5 nm}, Gd_{5 nm}Fe_{30 nm}, and Gd_{5 nm}Fe_{5 nm} multilayers, respectively. The experimental values obtained are 20, 16, 7, and 52 Ω, respectively. This extra resistance of the experimental values has various sources as we describe in the following points (new quantitative values will be given after the theoretical analysis).

Resistance of the interface. Of all the samples deposited for this work and others for similar studies, we always found that the resistance was larger for a larger number of interfaces. It has been suggested¹⁷ that the Gd close to the interface might be highly spin polarized, as a different phase to the bulk Gd. This contributes to a large spin scattering at the interface and therefore to a higher interface resistance (especially noticeable in the sample with 30 bilayers), as shown in the model below.

*Imbalance of the bridge caused by nonuniformities in the perpendicular current distribution.*¹¹ In the worst possible scenario more than 90% of the current will flow perpendicular to the mesas, following the model of Ref. 11. This is not the case for the arms without mesas where the value is ~20%. This clearly creates some imbalance of the bridge.

Different resistivity for different thickness. It has been shown in the past^{13,14} that the structure of the Gd layers depends on the thickness of the layer. This could change the resistivity of the Gd slightly for different thicknesses. This small effect is very difficult to estimate.

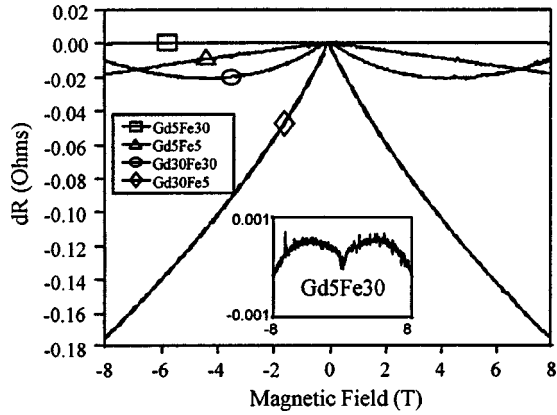


FIG. 4. Change in the resistance in CPP configuration for the four samples under study. As explained in the text, we do not plot MR to avoid the contribution of spurious resistance from the Cu contacts. The values of the total resistance are given in the text. The inset is the curve for $\text{Gd}_5\text{nm}-\text{Fe}_{30\text{nm}}$ sample with vertical scale expanded.

The results of the transport measurements at 20 K and up to 8 T are displayed in Fig. 4. We have plotted only the change of resistance instead of MR in order to avoid any contribution from the spurious resistance of the Cu contacts. The choice of 20 K as measuring temperature is not particularly critical; it is simply well below the compensation temperature of any of the samples. The behavior shown in Fig. 4 is surprisingly different from sample to sample, and not only in the value of dR , but also in shape as shown in the inset for sample $\text{Gd}_5\text{nm}-\text{Fe}_{30\text{nm}}$. The model introduced by Eerenstein *et al.*¹ of conductivity proportional to $\cos^2\varphi$ in Fe_3O_4 samples cannot explain the variety of results in these Gd/Fe multilayers with different thicknesses. In order to model the CPP transport in these sharp boundaries, we first have to understand how the magnetization is behaving with applied field, especially close to the boundary. The energy E of every boundary, from the middle of the Gd layer to the middle of the Fe layer, neglecting magnetostatic terms (with the field in the plane of the sample and the given dimensions of the mesas, even for $H=1$ T, the Zeeman energy is already three orders of magnitude larger than the magnetostatic energy) is¹²

$$E = E_{\text{Gd}}(\varphi_{\text{Gd}}, H) + E_{\text{Fe}}(\varphi_{\text{Fe}}, H) - A_{\text{int}} \cos(\varphi_{\text{Gd}} - \varphi_{\text{Fe}}), \quad (1)$$

where

$$E_X(\varphi_x, H) = \int_{\varphi(x=t/2)}^{\varphi(x=0)} [K \sin^2 2\varphi + HM_S \cos \varphi + A(d\varphi/dx)^2] d\varphi \quad (2)$$

is the energy from the middle of the layer X to the interface. A is the exchange energy, M_S is the saturation magnetization, H is the external field, t is the thickness of the layer, φ is the angle of every magnetic moment with the external field, A_{int} is the interface exchange coupling divided by the interatomic distance at the interface, and K is the cubic an-

isotropy constant of Fe. With the values given below, the Zeeman energy is considerably larger than the anisotropy energy for fields larger than the saturation field of Fe (~ 0.2 T), so the polycrystalline nature of the samples does not influence the final conclusions. φ_{Gd} and φ_{Fe} are the angle of Gd and Fe atom moments at the interface with respect to the external field, so the angle at the interface can be defined as $\varphi_i = \varphi_{\text{Gd}} - \varphi_{\text{Fe}}$.

The minimization of the energy E gives the direction of every magnetic moment with respect to the external field direction. The solution to this equation is analytical for one interface and infinite layers,¹² but requires numerical modeling for finite multilayers. We have performed this simulation using the following values: $A_{\text{Fe}} = 2.1 \mu\text{erg/cm}$, $A_{\text{Gd}} = 0.75 \mu\text{erg/cm}$, $A_{\text{int}} = -1 \mu\text{erg/cm}$, $K_{\text{Fe}} = 4.7 \times 10^5 \text{ erg/cm}^3$, $K_{\text{Gd}} \sim 0$, $M_S(\text{Fe}) = 1714 \text{ emu/cm}^3$, $M_S(\text{Gd}) = 1510 \text{ emu/cm}^3$. Following other authors,^{13,14} the value of $M_S(\text{Gd})$ in Gd/Fe multilayers is 75% of the bulk value, however, the qualitative final result is insensitive to this value. Figure 4 shows the result of the simulation for samples $\text{Gd}_5\text{nm}-\text{Fe}_{5\text{nm}}$ and $\text{Gd}_{30\text{nm}}-\text{Fe}_{30\text{nm}}$. The behavior of both with field is clearly different. For high fields the core of every layer in sample $\text{Gd}_{30\text{nm}}-\text{Fe}_{30\text{nm}}$, is aligned with the field and the magnetization forms a sharp domain wall close to the interface. When the layers are thinner, a higher field is required to create these domain walls (see the simulation for $\text{Gd}_5\text{nm}-\text{Fe}_{5\text{nm}}$). This is because the Zeeman energy of a thin layer is small in comparison with the exchange energy of a very narrow domain wall. In this case (thinner layers), the moments in a layer move towards (or against) the field as a block rather than creating a domain wall. $\text{Gd}_{30\text{nm}}-\text{Fe}_{30\text{nm}}$ is the only sample that shows such sharp domain walls close to the interface for high fields. The other three samples present a much sharper transition of the magnetization close to the interface for high fields. Therefore, for the samples $\text{Gd}_{30\text{nm}}-\text{Fe}_{5\text{nm}}$, $\text{Gd}_5\text{nm}-\text{Fe}_{30\text{nm}}$, and $\text{Gd}_5\text{nm}-\text{Fe}_{5\text{nm}}$, we can assume that the magnetization within each layer is uniform in the whole range from 0 to 8 T. In these three cases, only the angle at the interface φ_i changes with the field. With this simulation we can extract the angle at the interface Gd/Fe φ_i which are displayed in the inset of Fig. 6. Figure 5 does not include the top and bottom layers of the multilayer for clarity. Our simulations showed a slightly less sharp twisting of the magnetizations in these two layers and therefore they are less influential for the transport measurements, although they are key for the magnetization process of the multilayers as it was recently shown by Haskel *et al.*¹⁵

The simulation has periodic boundaries and therefore does not take into account any magnetostatic effect at the edges of the mesas. This is a good approximation despite the size of the mesas. The reason lies in the fact that in the experimental setup the windows of the SiO_2 around the mesas is much smaller than the mesas (3.5 μm versus 10 μm), therefore the edges do not influence the magnetization in the center. It is also important to realize that the layers have a quite different M_S , which implies that the magnetization cannot have any component perpendicular to plane because of the high magnetostatic energy that this would create.

Once we have characterized the behavior of the magnetization with the external magnetic field and in particular the angle at the interface, we need a quantitative model to predict the CPP transport through the interface for different fields. It is clear that a Gd/Fe multilayer is similar to a GMR multilayer but with the NM layer substituted by a FM layer. The spin transport in GMR multilayers is described by the Valet and Fert model.³ They demonstrated that in the normal situation of a spin-diffusion length much larger than the mean free path of the electron, the spin transport in mul-

tilayers could be described with a diffusion equation. They solved the equation in a general case of a multilayer [FM/NM]_n with the assumption of spin-dependent scattering at the interface and found an expression [Eqs. (41) and (42) in Ref. 3] to describe the contribution of the interface to the total resistance. Following the same terminology and analysis of Valet and Fert we can obtain a generalized expression of the interface resistance r_{SI} for multilayers [Gd/Fe]_n with thickness t_{Gd} and t_{Fe} , coupled antiferromagnetically:

$$r_{SI} = \frac{\rho_{Gd}^* \ell_{Gd} \rho_{Fe}^* \ell_{Fe} (\beta_{Gd} + \beta_{Fe})^2 + r_b^* \rho_{Gd}^* \ell_{Gd} (\beta_{Gd} + \gamma)^2 \coth[t_{Fe}/2\ell_{Fe}] + r_b^* \rho_{Fe}^* \ell_{Fe} (\beta_{Fe} - \gamma)^2 \coth[t_{Gd}/2\ell_{Gd}]}{r_b^* \coth[t_{Fe}/2\ell_{Fe}] \coth[t_{Gd}/2\ell_{Gd}] + \rho_{Gd}^* \ell_{Gd} \coth[t_{Fe}/2\ell_{Fe}] + \rho_{Fe}^* \ell_{Fe} \coth[t_{Gd}/2\ell_{Gd}]} \quad (3)$$

All the parameters in Eq. (3) are defined as in Ref. 3: β is a spin asymmetry coefficient for the spin conduction, defined as $\rho^{\uparrow(\downarrow)} = 2\rho^* [1 - (+)\beta]$, so the total resistivity is $\rho = (1 - \beta^2)\rho^*$. The spin-diffusion length is represented by $l = (D\tau_{SF})^{1/2}$ where τ_{SF} is the spin-flip time and D the diffusion constant $D = v_F \lambda$ with v_F the Fermi velocity and λ the mean free path of the electrons. The parameters r_b^* and γ determine the spin-dependent scattering at the interface and they are defined as

$$r_{\uparrow(\downarrow)} = 2r_b^* [1 - (+)\gamma]. \quad (4)$$

For the very high field limit, when all the layers are perfectly aligned (and $\varphi_i = 0$), expression (3) is only modified by making the following replacements: $(\beta_{Gd} + \beta_{Fe})^2$ by $(\beta_{Fe}^2 - \beta_{Gd}^2)$ and $(\beta_{Gd} + \gamma)^2$ by $(\beta_{Gd} - \gamma)^2$. When one of the layers becomes nonferromagnetic, e.g., when $\beta_{Gd} = 0$, expression (3) becomes Eq. (41) in Ref. 3.

In the case we are studying from 0 to 8 T, the total resistance of each bilayer of the heterostructure (with two interfaces per bilayer) is given by

$$R = (1 - \beta_{Gd}^2)\rho_{Gd}^* + (1 - \beta_{Fe}^2)\rho_{Fe}^* + 2(1 - \gamma^2)r_b^* + 2r_{SI}. \quad (5)$$

These expressions describe the behavior of a multilayer when the layers are coupled antiferromagnetically ($\varphi = 180^\circ$ at the interface) or when they are parallel ($\varphi = 0^\circ$). We assume the spin-dependent scattering at the interface is a maximum in the antiferromagnetic state $\varphi = 180^\circ$ and it will be reduced as the external field is increased and therefore the angle at the interface φ_i is reduced. Therefore we can assume that the asymmetry parameter γ of Eq. (4) depends on the angle of the interface as $\gamma = \gamma_0 \cos^2 \varphi_i$. If the layers are rotated 90° the spin asymmetry goes to zero and Eq. (4) is reduced to $r_{\uparrow(\downarrow)} = 2r_b^*$, which corresponds to the situation in which both spin up and spin down have to adapt the same angle (90°) to go through the interface to the next layer. We should emphasize here that this dependence on the angle is only valid when the interface angle is changing but the mag-

netization of all the atoms in each layer have roughly the same angle with the external field, so they all move together and no domain wall is formed close to the interface.

The dependence of γ on φ_i affects the last two terms of Eq. (5). We can now use the angles at the interface for the different samples calculated previously and calculate the

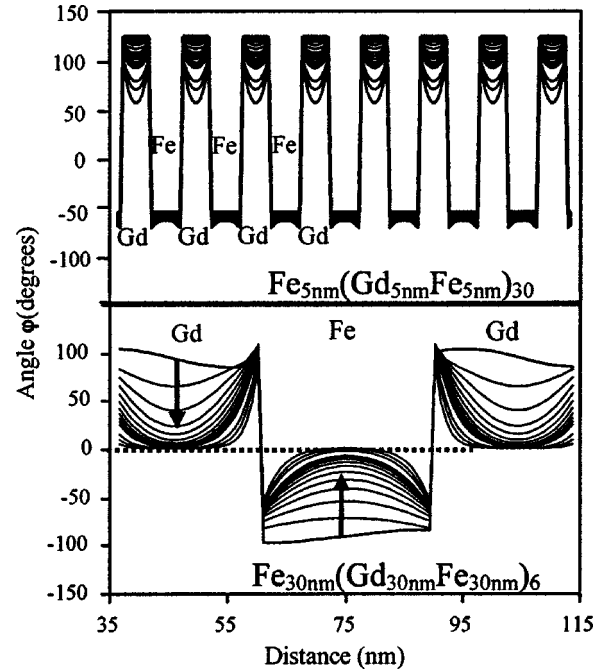


FIG. 5. Variation of the angle φ of the magnetization in $Fe_{5\text{ nm}}(Gd_{5\text{ nm}} - Fe_{5\text{ nm}})_{30}$ and $Fe_{30\text{ nm}}(Gd_{30\text{ nm}} - Fe_{30\text{ nm}})_{6}$ samples versus field. The solid arrows by the curves indicate the direction of increasing field, from 0 to 1 T every 0.1 T and 1.5, 2.0, and 3.0 T. This figure plots the direction of the moment within one bilayer of the multilayer versus field. The line $\varphi = 0^\circ$ represents the direction of the applied field. Note that sample $Fe_{30\text{ nm}}(Gd_{30\text{ nm}} - Fe_{30\text{ nm}})_{6}$ holds domain walls by the interface while in samples with thinner layers, every layer moves homogeneously with respect to each other. The initial direction of the layers (at $H = 0$ T) is determined by the anisotropy axis of Fe induced during the deposition.

change in R when the external field is increased. The following values accurately predict the experimental results: $\rho_{\text{Gd}} = 110 \mu\Omega \text{ cm}$, $\rho_{\text{Fe}} = 8 \mu\Omega \text{ cm}$, $\beta_{\text{Gd}} = 0.4$, $\beta_{\text{Fe}} = 0.45$, $\ell_{\text{Gd}} = 100 \text{ nm}$, $\ell_{\text{Fe}} = 60 \text{ nm}$, $\gamma_0 = 0.2$, and $r_b^* = 5.8 \times 10^{-15} \Omega/\text{m}^2$. All the values are very similar to those used in previous works¹⁶ but r_b^* which is one order of magnitude higher than the standard value used for GMR multilayers. This gives us the following total resistances for the multilayers: 12.5, 11.8, 5, and 22 Ω for the samples $\text{Gd}_{30 \text{ nm}}\text{Fe}_{30 \text{ nm}}$, $\text{Gd}_{30 \text{ nm}}\text{Fe}_{5 \text{ nm}}$, $\text{Gd}_{5 \text{ nm}}\text{Fe}_{30 \text{ nm}}$, and $\text{Gd}_{5 \text{ nm}}\text{Fe}_{5 \text{ nm}}$, respectively, which are of the same order of magnitude as the experimental values. The large value of r_b^* can be argued to be due to the fact that in Gd/Fe layers the spin of the electrons has to flip from one layer to the other, while in GMR multilayers the spin diffuses from the FM layer to the NM layer. It can also be due to the fact the spin polarization of the Gd close to the interface could be quite high.¹⁷ There is still a small mismatch in the calculated values of the resistances with the measured values that is attributed to small differences in the multistep lithographic process or to small changes in the resistivities of the layers for different thicknesses.^{13,14}

The change of R from Eq. (5) with field is displayed in Fig. 6 for the different samples. As expected, the curve for sample $\text{Gd}_{30 \text{ nm}}\text{Fe}_{30 \text{ nm}}$ fits with the experimental result only for small fields. For larger fields, domain walls are generated close to the interface (see Fig. 5) and the spin transport in the heterostructure is different: most of the multilayer is aligned with the field and there are domain walls at every interface that create a positive resistance.^{18,19} This effect has been predicted recently theoretically by Inoue *et al.*²⁰ In fact a multilayer such as $\text{Gd}_{30 \text{ nm}}\text{Fe}_{30 \text{ nm}}$, with domain walls of a controllable size, could be an ideal system to understand the controversial subject of the magnetoresistance of domain walls. The flat region around zero field in $\text{Gd}_{30 \text{ nm}}\text{Fe}_{5 \text{ nm}}$ and $\text{Gd}_{5 \text{ nm}}\text{Fe}_{30 \text{ nm}}$ samples is not present in the experimental results. This flat region is a consequence of the fact that for small fields, the thicker layer (the one with larger volume of magnetic moment) aligns with the field and the thin layer aligns antiparallel to it. This situation is stable until the Zeeman energy of the antiparallel layer is too large and the whole heterostructure starts to twist. The absence of the flat region in the experimental curves is probably due to small

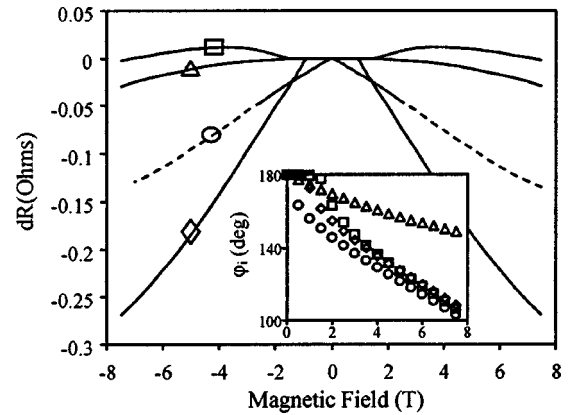


FIG. 6. Calculated change in the resistance with field following Eq. (5), for the four samples under study. The curves are labeled with the same symbols as in Fig. 4. The inset shows the calculated angle of the interface φ_i for each sample versus field. This angle is the input to the generalized formula (3) from Valet and Fert model. The dashed line in sample $\text{Gd}_{30 \text{ nm}} - \text{Fe}_{30 \text{ nm}}$ indicates the region where the model might not be valid anymore because of the formation of domain walls at the interface.

long-range “orange peel” roughness at the interfaces¹³ that facilitates the magnetization process.

In conclusion, we have characterized spin transport through a sharp antiferromagnetic interface by extending the Valet and Fert model for GMR multilayers with spin asymmetric scattering at the interface dependent on the angle at the interface. Eerenstein *et al.*¹ assumed a model of conductivity proportional to $\cos^2 \varphi$ with no spin-dependent scattering at the interface in antiferromagnetic boundaries of Fe_3O_4 . We found that this model could not explain our results in Gd/Fe, where just a change in the relative thickness of the layers dramatically affects the magnetoresistance. We have assumed that the spin-diffusion length does not depend on the angle of the interface. We found this was a good approximation up to 8 T of external field. These kinds of heterostructures may also be a good system to understand what the spin is doing close to the interface when the angle at the interface φ_i is smaller than 180° : spin flip or precession plus spin flip.

We acknowledge the generous suggestions from Dr. A. Fert and EPSRC for financial support.

*Email address: jlp31@cam.ac.uk

¹W. Eerenstein, T.T.M. Palstra, S.S. Saxena, and T. Hibma, Phys. Rev. Lett. **88**, 247204 (2002).

²M.A.M. Gijs, S.K.J. Lenczowski, and J.B. Giesbers, Phys. Rev. Lett. **70**, 3343 (1993).

³T. Valet and A. Fert, Phys. Rev. B **48**, 7099 (1993).

⁴D. Haskel, G. Srager, J.C. Lang, J. Pollmann, C.S. Nelson, J.S. Jiang, and S.D. Bader, Phys. Rev. Lett. **87**, 207201 (2001).

⁵J. Landes, Ch. Sauer, B. Kabius, and W. Zinn, Phys. Rev. B **44**, 8342 (1991).

⁶J.P. Andrés, L. Chico, J. Colino, and J.M. Riveiro, Phys. Rev. B **66**, 094424 (2002).

⁷V.L.B. de Jesús, I.S. Oliveira, P.C. Riedi, and A.P. Guimarães, J. Magn. Magn. Mater. **212**, 125 (2000).

⁸O.F.K. McGrath, N. Ryzhanova, C. Lacroix, D. Givord, C. Feron, C. Miramond, G. Saux, S. Young, and A. Vedyayev, Phys. Rev. B **54**, 6088 (1996).

⁹K. Engl, W. Brunner, and J. Zweck, J. Phys.: Condens. Matter **14**, 10033 (2002).

¹⁰M. Vaezzadeh, B. George, and G. Marchal, Phys. Rev. B **50**, 6113 (1994).

¹¹S.K.J. Lenczowski, R.J.M. van de Veerdonk, M.A.M. Gijs, J.B. Giesbers, and H.H.J.M. Janssen, J. Appl. Phys. **75**, 5154 (1994).

¹²H. Sijlstra, IEEE Trans. Magn. **MAG-15**, 1246 (1979).

- ¹³N. Ishimatsu, H. Hashizume, S. Hamada, N. Hosoi, C.S. Nelson, C.T. Venkataraman, G. Srajer, and J.C. Lang, *Phys. Rev. B* **60**, 9596 (1999).
- ¹⁴W. Hahn, M. Loewenhaupt, Y.Y. Huang, G.P. Felcher, and S.S.P. Parkin, *Phys. Rev. B* **52**, 16 041 (1995).
- ¹⁵D. Haskel, G. Srajer, Y. Choi, D.R. Lee, J.C. Lang, J. Meerss-chaut, J.S. Jiang, and S.D. Bader, *Phys. Rev. B* **67**, 180406(R) (2003)
- ¹⁶A. Fert and H. Jaffrès *Phys. Rev. B* **64**, 184420 (2001).
- ¹⁷H. Tang, D. Weller, T.G. Walker, J.C. Scott, C. Chapeert, H. Hoster, A. W. Pang, D. S. Dessau, and D. P. Pappas, *Phys. Rev. Lett.* **71**, 444 (1993).
- ¹⁸P.M. Levy and S. Zhang, *Phys. Rev. Lett.* **79**, 5110 (1997).
- ¹⁹J.L. Prieto, M.G. Blamire, and J.E. Evetts, *Phys. Rev. Lett.* **90**, 027201 (2003).
- ²⁰J. Inoue, H. Itoh, S. Mitani, and K. Takanashi, *Phys. Rev. B* **68**, 094418 (2003).